# Smartphone Positioning with Radio Measurements from a Single WiFi Access Point

Maurizio Rea
maurizio.rea@imdea.org
IMDEA Networks Institute &
University Carlos III of Madrid
Madrid, Spain

Traian Emanuel Abrudan
traian.abrudan@nokia-bell-labs.com
Nokia Bell Labs
Dublin, Ireland

Domenico Giustiniano
domenico.giustiniano@imdea.org
IMDEA Networks Institute
Madrid, Spain

Holger Claussen
holger.claussen@nokia-bell-labs.com
Nokia Bell Labs
Dublin, Ireland

Veli-Matti Kolmonen
veli-matti.kolmonen@
nokia-bell-labs.com
Nokia Bell Labs, Espoo
Southern Finland, Finland

## ABSTRACT

Despite the large literature on localization, there is no solution yet to localize a commercial off-the-shelf smartphone device using radio measurements from a single WiFi AP. We present *SPRING*, Smartphone Positioning with Radio measurements from a sINGle wifi access point. SPRING exploits Fine Time Measurements (FTM) and Angle of Arrival (AOA) extracted from commercial chipsets exploiting the specifications of the recent 802.11-2016 and the 802.11ac amendment to combine distance and direction from the AP to the client for positioning. Our system has the potential to bring indoor positioning to homes and small businesses which typically have a single access point. We exploit physical layer (PHY) information to detect the number of paths and their directions. We use this information to derive a new method for filtering ranging measurements obtained with the FTM protocol. We achieve sub-meter distance estimation accuracy eliminating the adverse effect of multipath in FTM using calibrated inputs from Channel State Information (CSI). Our evaluation in indoor scenarios in multipath rich environments demonstrates that the combination of AOA estimation and the proposed FTM refinement approach can locate a Google Pixel 3 smartphone with a median positioning error of 0.9-2.15 m through an area comparable to typical flat sizes.

## CCS CONCEPTS

• **General and reference** → **Measurement**; • **Hardware** → **Wireless devices**; **Hardware test**; *Digital signal processing*; *Networking hardware*; • **Networks** → *Network experimentation*;

## KEYWORDS

Localization system; Channel State Information; Fine Time Measurements; Angle of Arrival;

**ACM Reference Format:**
Maurizio Rea, Traian Emanuel Abrudan, Domenico Giustiniano, Holger Claussen, and Veli-Matti Kolmonen. 2019. Smartphone Positioning with Radio Measurements from a Single WiFi Access Point. In *International Conference On Emerging Networking Experiments And Technologies (CoNEXT '19), December 9–12, 2019, Orlando, FL, USA.* ACM, New York, NY, USA, 7 pages. https://doi.org/10.1145/3359989.3365427


*CoNEXT '19, December 9–12, 2019, Orlando, FL, USA*

ACM ISBN 978-1-4503-6998-5/19/12…$15.00
https://doi.org/10.1145/3359989.3365427

## 1 INTRODUCTION

Indoor positioning has attracted a lot of attention from the research as well as industry communities. Due to the limitation and complexity of the indoor environment, the problem of bringing indoor positioning to homes and small businesses which typically have a single Access Point (AP) remains open. Accurate indoor positioning can be achieved using different approaches such as the signal strength [1, 3, 7, 13, 23], Angle of Arrival (AOA) [6, 12, 19, 22], time-based ranging [5, 14, 16, 21] or combining WiFi signals with inertial sensors as found in smartphones [15, 17]. While localizing a client with a dense network of APs has been solved [12], early attempts to operate with a single AP assume that the WiFi chipset in the AP can continuously change its frequency of operation [2, 20]. However, commodity smartphones do not have this feature, which is not supported by any 802.11 standard. [15] operates with a single AP, but requires the access to inertial sensors of smartphones and extensive manual calibration per user. All the above factors limit the deployment of these approaches at larger scale.

In this work, we introduce SPRING, Smartphone Positioning with Radio measurements from a sINGle wifi access point. First, it takes advantage of the 802.11ac standard, exploiting in 80 MHz bandwidth the PHY layer information called Channel State Information (CSI), obtained from multiple antennas in a single AP. These chipsets come with problems of calibration before being used to extract high-resolution AOA. Second, recently, IEEE 802.11-2016 standardized [10] the FTM protocol to supports time-based WiFi ranging techniques. So far, there have been few studies of such ranging system, with limit investigation of methods to alleviate the

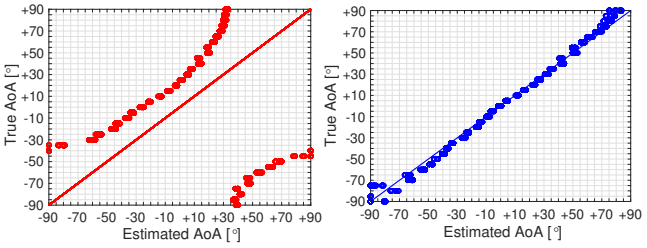


(a) Before phase calibration (b) After phase calibration

**Figure 1: MUSIC estimations in the anechoic chamber.**

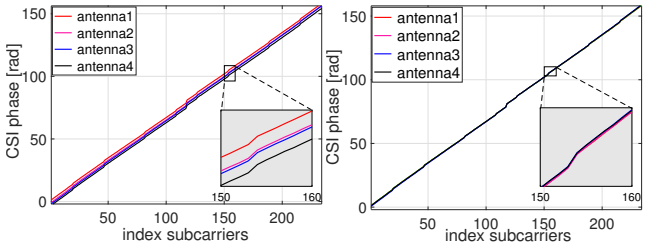


(a) Before phase calibration (b) After phase calibration

**Figure 2: A snapshot of CSI unwrapped phases for each antenna, at $0^\circ$.**

multipath. Based on corrected input data, SPRING measures the angle and the distance from a single AP to a commercial off-the-shelf smartphone (Google Pixel 3), showing for the first time the feasibility to locate a smartphone in typical indoor environments only with measurements performed by the single AP.

The paper is organized as follows. First, we describe how to obtain AOA estimations from CSI. We then discuss our proposed solution to avoid the phase calibration issue related to the WiFi chipset, showing how well it alleviates the phase error. Next, as FTM is a new feature from the 802.11 standard, no model to treat the noise has been presented so far. We analyze the key factors and parameters that affect the ranging performance using the FTM protocol and introduce a model to treat the noise in FTM measurements. We mitigate the impact of multipath in FTM measurements, developing an estimator that receives calibrated inputs from CSI. We also compare our estimator with other techniques, showing performance improvements. Finally, we evaluate SPRING and we demonstrate using only commodity hardware that the target device can be localized across two different experimental testbeds with a median accuracy between 0.9 and 2.15 meters in areas up to 125 $m^2$.

## 2 CHANNEL STATE INFORMATION

This section presents how to obtain CSI measurements with the proposed hardware, presented in Section 5.1, and how to estimate the AOA.

### 2.1 From CSI to AoA estimate

We obtain the AoA from the CSI, available in the PHY layer. The reported CSI is a matrix containing one complex number per subcarrier and per received antenna at the AP. We use multiple signal classification (MUSIC) algorithm [18] to identify the strongest angle of arrival. This technique performs the subspace decomposition of the autocorrelation matrix.

### 2.2 Measurements in Anechoic Chamber

Our first experimental setup consists of a custom lab prototype as AP and a raspberry Pi with an external dongle for supporting the 802.11ac standard configured as STA. We start with the anechoic chamber as indoor scenario, in order to avoid multipath. More in details, the STA is connected to the AP through channel 112 at 5.56 GHz as carrier frequency. The device gives the ability to configure the number of subcarriers ($N_s$) sending data, typically used by the Compressed Beamforming Feedback Matrix in 802.11ac for beamforming. We select the highest number of subcarriers (234), which allows us to get the highest resolution in the analysis of the spectrum. In this setup, we fix the STA in the middle of the room and rotate the AP in order to span an angle of $\pi$, from $\frac{-\pi}{2}$ to $\frac{+\pi}{2}$, where $0^\circ$ corresponds to the normal direction of the antenna array elements, which are placed as Uniform Linear Array (ULA) with a distance of $\lambda/2$ between antennas. More specifically, we conduct 36 experiments, every $5^\circ$, and for each of them we collect around 165 CSI samples. Fig. 1a shows the true AOA versus the estimated AOA in degrees, and illustrates a calibration issue that introduces a bias in all estimations. This phenomenon is due to a phase shift in each antenna for all $N_s$ subcarriers.

### 2.3 Phase Calibration

In this subsection, we propose a solution to correct the bias shown in the previous subsection, without involving any theoretical model. The principle behind is that, due to the far field assumption of a received single path CSI, at $0^\circ$ measurements all the phases are supposed to be overlapped, for all antennas and over all $N_s$ subcarriers. As shown in Fig. 2a, the CSI unwrapped phases of all 4 antennas are shifted, and for this reason we estimate another AOA ($\sim 24^\circ$).

To correct this shift, we evaluate the phase difference between all antennas and all sub-carrier with respect to the measurements at the first antenna at $0^\circ$ only, given by the vector

$$\Delta\varphi_m = \angle(\mathbf{CSI}_m \cdot \overline{\mathbf{CSI}}_1), \tag{1}$$

where $m$ is the antenna index and $\overline{\mathbf{CSI}}_1$ is the complex conjugate of vector $\mathbf{CSI}_1$.

For each antenna and subcarrier, we then calibrate the CSI as follows:

$$\textbf{calibrated CSI}_m = \mathbf{CSI}_m \cdot e^{-j\Delta\varphi_m}. \tag{2}$$

Doing so, we obtain the required overlap, as shown in Fig. 2b, where the difference between the unwrapped phases of all antennas is close to zero. In Fig. 3, the solid line shows the evolution of the median of $\Delta\varphi$ for each antenna over the set of samples $\mathcal{S}$ (one sample is collected per packet). Based on Eq. 2, the median of $\Delta\varphi_1$ is 0 for each packet, and the median over all packets of the median of $\Delta\varphi$ across all subcarriers is

$$\Delta\varphi_m = [0, -1.976, -2.532, 2][rad], with\ m \in \{1, .., 4\}.$$

Fig. 1b shows the true AOA versus the "calibrated" AOA estimation, highlighting the benefit of the proposed CSI phase calibration. Doing so, the estimated AOA well matches the true AOA. This procedure is necessary only once.

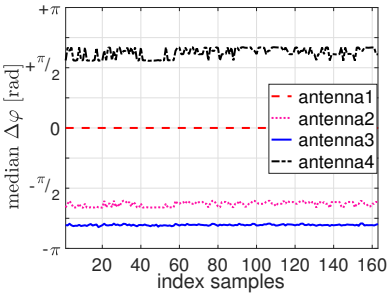


**Figure 3: Median of $\Delta\varphi$ for each antenna.**

## 3 FINE TIME MEASUREMENTS

In this section we provide the background on the FTM protocol of the IEEE 802.11-2016 standard and we model the detected FTM noise.

### 3.1 IEEE 802.11mc Background

IEEE 802.11-2016 standardized the FTM protocol to enable a pair of WiFi chipsets to estimate the distance between them. A FTM initiator (FTMI) is a STA that initiates the FTM process by sending a FTM Request to a corresponding AP. An AP that supports the FTM procedure as a responding device is called a responder (FTMR). If the AP agrees to perform the measurements, it starts to send FTM message and wait for its ACK. The Round Trip Time (RTT) is estimated based on the transmission timestamp of the FTM message and the reception timestamp of its ACK. In the computation, the protocol subtractes STA processing time from the total round trip time. Yet, as all localization systems performing active wireless measurements, data retransmissions are possible due to collisions. It follows that interference tends to increase the time required to obtain a sufficient number of messages for localization.

### 3.2 FTM Sources of Noise

Signal propagation in rich indoor environments is subject to multipath effects where multiple coherent copies of the transmitted signal arrive at the receiver over different reflected paths. It is even possible that the direct component is severely attenuated and the signal is received mostly over reflected paths. Since signals that travel over reflected paths will take longer time to arrive at the receiver, they introduce an error in the distance estimation when considering the time-of-flight.

We define the following function $y$ for a path $i \in \mathcal{L}$, where $\mathcal{L}$ denotes the set of paths to the target station (FTMI):

$$y = \log_{10}\left(d_i\right) + \mathcal{N}(0, \sigma_{\mathcal{N}}) \qquad d_i \geq d_0. \tag{3}$$

$\mathcal{N}(0, \sigma_{\mathcal{N}})$ represents an additive Gaussian noise $\mathcal{N}$, with a standard deviation $\sigma_{\mathcal{N}}$, and $d_0$ is equal to 1 m. This expression is inspired by the path loss model with the log-normal distribution that represents the shadowing effect.

Now, let $\mathcal{S}$ be the set of samples. We express the generic FTM sample as:

$$d_{i,s} \qquad i \in \mathcal{L}, s \in \mathcal{S}. \tag{4}$$

Based on the model in eq. (3), in Section 4.1 we will introduce the first path estimator $f$ to mitigate the effects of the main sources of noise in the channel. The estimator will operate in the log domain, i.e., $log_{10}(d_{i,s})$.

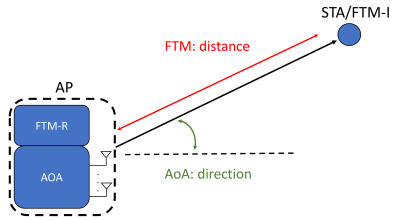


**Figure 4: Hybrid FTM/AOA approach.**

Furthermore, the RTT for short distances returns negative values, underestimating the true distance. Since multipath can lead to longer paths, we believe that this effect, that allows the signal to arrive earlier than expected, is due to a post-processing in the firmware. In this paper, we correct the offset using the experimental value in [9]. However, even after correcting the fixed offset, the ranging system may give $d_{i,s}$ smaller than $d_0$. As such, we add a constant factor for the purpose of operating in the log domain, such that it is larger than $d_0$ for a sequence of samples.

## 4 HYBRID FTM/AOA SYSTEM

In Fig. 4 we show the high-level illustration of our hybrid FTM/AOA localization system. While being associated to the WiFi chipset performing AOA measurements, the STA sends FTM requests to the FTMR (using a different WiFi chipset). This is possible since the protocol allows the initiator to exchange FTM packets without the need to be associated with a WiFi AP. We collect AOA and distance measurements from AP AOA and FTMR, respectively, and post-process the results.

### 4.1 FirstPath Estimator for FTM

This subsection describes in details the estimator $f$ of the first path.

In eq. (4), each FTM sample $d_{i,s}$ is affected by a distance bias caused by the absence or presence of multipath. Grouping together the samples with the same bias results in a finite Gaussian Mixture Model (GMM) in the log domain with a small number of modes. One of these modes corresponds to the samples received through the direct path, while the others correspond to the samples received through to any of the reflected paths.

Then, knowing the number of estimated paths, we can separate all the Gaussian components, and the median or the mean of the first Gaussian would be a reliable estimator of the direct path's distance. For this purpose, we exploit the PHY layer information. But we do not invoke MUSIC algorithm as we do for AOA estimation. In fact, even in a single path scenario, the AOA MUSIC spectrum might present side lobes and furthermore, in the presence of multipath, the incoming signals are coherent and therefore the rank of the covariance matrix does not increase in order to be able to separate them. Consequently, having two incoming paths well separated in angular domain, we might only detect a single path. We instead resort to the Matrix Pencil Method (MPM) [8]. Knowing that the multipath channels are usually modeled in time-domain as a weighted sum of delayed impulse functions, for each antenna $a$, let $L_a$ be the number of delayed paths, and $\tau_{l,a}$ and $h_{l,a}$ the propagation delay and the complex gain of the l-th path, respectively. MPM uses as input the calibrated CSI values from eq. (2), it operates on the frequency response of the channel and it calculates

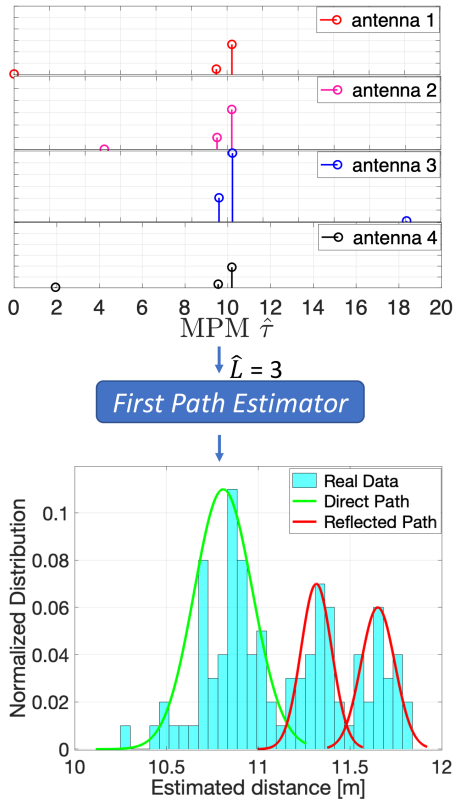


**Figure 5: Example of the estimator $f$ for a real case where the real distance is 10.73 m. The number of paths, $\hat{L}$, is the mode of the estimations provided by the Matrix Pencil Method for each antenna, and it is given as input to the estimator $f$ that calculates only the mean of the first log-Gaussian.**

with high accuracy the estimated values $\hat{L}_a, \hat{\tau}_{l,a}$ and $\hat{h}_{l,a}$. We then calculate the estimated number of paths as $\hat{L} = Mo(\hat{L}_1, \hat{L}_2, \hat{L}_3, \hat{L}_4)$ where $Mo$ indicates the most frequent value (mode).

Fig. 5 shows an example of a real case. We observe that the estimator $f$ estimates the parameters of the components of the Gaussian mixture very well: the direct path has a traveled distance of 10.73 m and the estimated mean of the direct path's distribution is equal to 10.82 m. It follows that we are able to estimate the distance of the direct path with an error of only 0.09 m. In Section 5 we show a comparison between the proposed filter and other metrics.

## 4.2 Deployment Scenarios

We perform experiments in two indoor testbeds, namely Testbed I and II. Both are office environments and the maps are shown in Fig. 6. Testbed I, in Fig. 6a, covers a surface of almost 65 $m^2$. We use 27 selected locations (marked as cross) to test our system, and the propagation is mainly over a line-of-sight (LOS) path. Deploying a single AP, the number of links is equal to the number of target STA locations. Testbed II is depicted in Fig. 6b. It covers a space of around 125 $m^2$ and the UE is placed in 35 different positions. In Testbed II, a mixture of LOS and non-line-of-sight (NLOS) wireless links are present. Testbed II also contains several obstructions, including concrete walls and tables (yellow boxes in Fig. 6b) and it is surrounded by glasses. All experiments are conducted with other

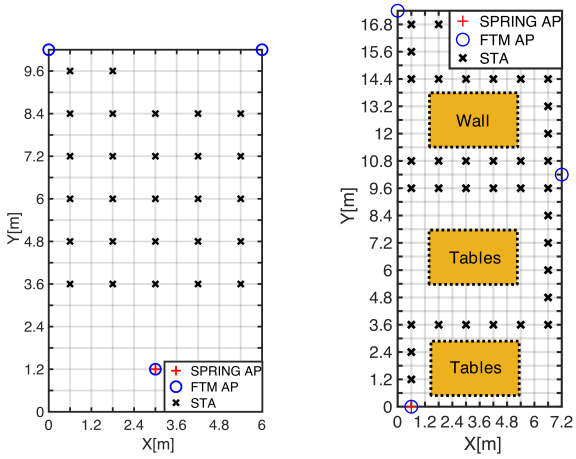


**(a) Testbed I.** **(b) Testbed II.**

**Figure 6: Testbeds to assess the direction, ranging and positioning capabilities of SPRING and baseline. Yellow box in Testbed II corresponds to blockage.**

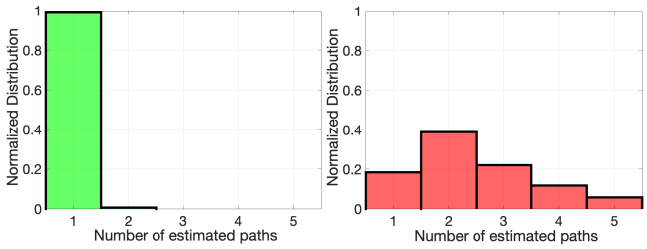


**(a) Testbed I.** **(b) Testbed II.**

**Figure 7: Normalized histograms of the number of estimated paths for Testbed I and II.**

active WiFi networks in the neighborhood. The PHY information are obtained on a fixed frequency channel of the 5 GHz band. For the evaluation of our system SPRING we deploy a single AP ('SPRING AP', red marker in Fig. 6), while for the evaluation of the proposed baseline we deploy three FTM-Rs ('FTM AP', blue circle in Fig. 6).

Furthermore, we highlight the difference in the scenarios complexity showing the number of estimated paths, using MPM, in Fig. 7. In Testbed I MPM estimates a single path almost 100% of the time, while in Testbed II it estimates a variable number of paths (from 1 to 5), due to the mixture of LOS and NLOS wireless links.

# 5 EVALUATION

In this section, first we introduce the experimental platform and then we analyze the performance of the AOA estimator, our proposed method for computing ranges and finally positioning of the STA in Testbed I and II. We deploy the Google Pixel 3 as target STA in all marked positions, shown in Fig. 6.

## 5.1 Experimental Platform

An illustration of the commodity hardware we use for the AP is shown in Fig. 8. The AP is composed by two different commodity chipsets (although we envision that, in the future, manufacturers will implement them in the same chipset). As mentioned in Section 4, the STA is associated to the chipset performing AOA, while FTM

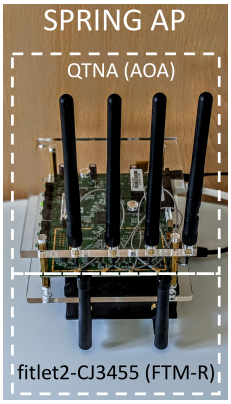


**Figure 8: SPRING AP used for measurements.**

does not require association of the STA. Therefore, it is possible to use the STA for both type of measurements. Three fundamental components are needed to deploy SPRING: a multi-antennas AP which enables collection of MIMO CSI, the FTM-R and the FTM-I, described in details in what follows. In order to collect CSI we use a QHS8405S4-RDK device, the Quantenna (QTNA) 4x1 Uniform Linear Array (ULA). QTNA supports PCIe, RGMII and 802.11a/n/ac protocol. The frequency range is from 5.15 GHz to 5.85 GHz and it supports 20/40/80 MHz bandwidth. QTNA enables rapid collection of precise high-order MIMO channel state information (CSI). The spatial diagnostics interface is supported on QTNA's BBIC4 based platform and it supports extracting up to 4x1 channels with bandwidth up to 80MHz, with CSI data from the driver accessed over a TCP socket. Any WiFi device can be used as the STA.

Regarding the FTM protocol, we choose the fitlet2-CJ3455 platform as responder (FTM-R) since it is an integrated solution in compact form, which includes the WiFi Intel 8265 chipset. We use the WiFi Indoor Location Device (WILD) configuration tool which enables all the configuration files for a FTMR.

As STA, we use the Google Pixel 3 phone with Android Pie (API Level 28) that supports the FTM protocol. The phone operates as FTMI for time measurements. The device must have location-based services enabled at the system level to access the FTM protocol. We use the android-WifiRttScan application to initiate the measurements. We modify its code to facilitate the data collection, and we configure it to receive a distance measurement per packet. Its main activity lists all APs using the WifiManager. By selecting an AP that supports FTM-R, another activity is launched and RangingRequest initiated via the WifiRttManager. The activity displays and stores many of the details returned from the FTMR including the distance reported between the AP and the smartphone.

## 5.2 AOA

We collect CSI data once the phone Google Pixel 3 is associated to the QTNA device. We estimate the AOA according to the methodology presented in subsection 2.1. For the estimation of the strongest path we consider the highest peak in the MUSIC spectrum. We then evaluate the AOA estimation error in Testbed I and II. From Fig. 9a we see the Empirical Cumulative Distribution Function (ECDF) of the AOA error in degrees. Estimating the strongest path does not mean we are always able to estimate the direct path: the median

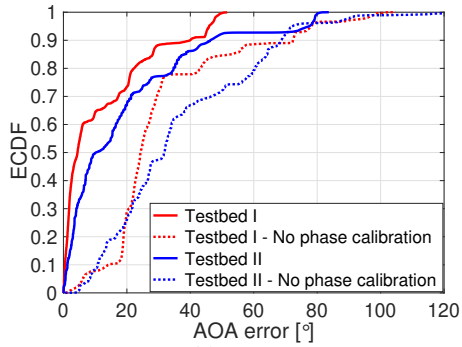


**(a) AOA.**

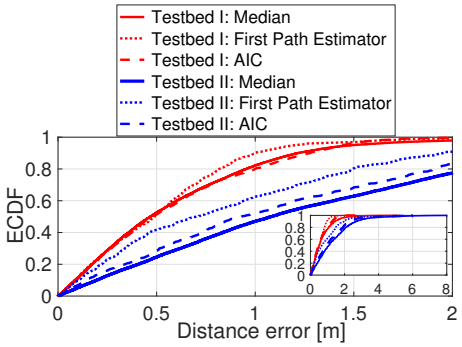


**(b) Distance.**

**Figure 9: ECDF of AOA estimation error in degrees with and without phase calibration (9a) and distance estimation error (9b) for our estimator compared to the median and AIC.**

and 80-percentile error are around 4.8° and 21° for Testbed I, respectively, while 14° and 36.5° for Testbed II. As shown in Fig. 9a, the error is reduced significantly with respect to a naive approach that considers the estimation of AOA without calibration.

## 5.3 Distance

In order to collect FTM measurements, the FTM-R sends FTM message to the phone and waits for the ACK. For this evaluation, we compute the distance estimation error with $M = 20$ samples for each link. Fig. 9 shows the ECDF of the ranging errors, for Testbed I and II. We obtain a median error of 0.49 m and an 80-percentile error of 0.86 m in Testbed I, while in Testbed II a median and 80-percentile error of 0.73 m and 1.5 m, respectively. As shown in Fig. 9b, we also compare the obtained results with both the median and the Akaike Information Criterion (AIC). The latter is commonly applied to identify the optimal number of clusters in GMM. We use the lowest AIC to infer the optimal number of paths [11] and then we use the path with the least positive mean as ranging estimate. Furthermore, the results shown in Fig. 9 highlight the difference on the scenarios complexity. In fact, in Testbed I where the target is in LOS with the AP, the difference between the proposed first path estimator and the simple median is not so relevant. In Testbed II the complexity increases having a mixture of LOS and NLOS wireless links, and so our solution greatly outperforms other estimators.

## 5.4 Positioning

In addition to the direction and ranging error, we also study the localization error. We define a coordinate system on a two-dimensional

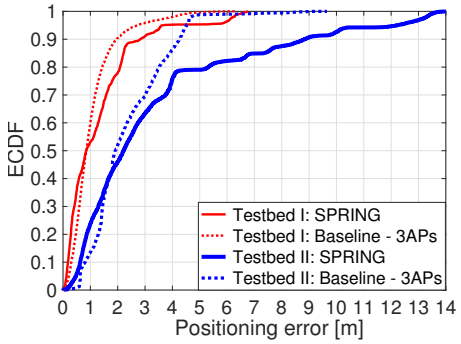


**Figure 10: Positioning error in Testbed I and II. Solid lines indicate SPRING, while dashed lines correspond to the baseline.**

map. Considering a single AP system, let $s = (x_{AP}, y_{AP})$ be the position of the AP, $\hat{d}$ the estimate of the distance from AP to the target and $\hat{\theta}$ the estimated direction between the AP and the target. We find the coordinates of the estimated position as follows:

$$\hat{p} = (\hat{x}, \hat{y}) = (x_{AP} + \hat{d} \cdot \cos\hat{\theta}, y_{AP} + \hat{d} \cdot \sin\hat{\theta}). \quad (5)$$

We study the position accuracy of our proposed system, SPRING, and we compare the obtained results with a baseline composed by three FTM APs. We consider this a fair comparison, as we aim to compare the performance with the minimum number of APs needed to perform positioning: SPRING needs only one AP, while 3 FTM APs are required for multilateration. For the latter, using the estimated distance from each FTM-R, we make an initial position estimate with the Linear Least Squares (LLS) multilateration algorithm. Then the algorithm makes use of the Non-Linear Least Squares (NLLS) technique to compute the position from this initial value. We summarize the results in Fig. 10, where solid lines indicate SPRING, while dashed lines correspond to the baseline. For Testbed I, SPRING achieves a median and 80-percentile positioning error of about 0.9 m and 2 m, respectively, while 2.15 m and 5 m for Testbed II. On the other hand, we observe that the baseline system accuracy tends to increase compared with SPRING, above 60 percentile. In fact, for Testbed I, the baseline achieves a median and 80- percentile positioning error of about 0.9 m and 1.4 m, respectively, while 2 m and 3.5 m for Testbed II. The reason is that, for a given deployment scenario, the density of APs plays an important role, avoiding performance degradation as the distance from the AP increases. Nevertheless, SPRING, with just one AP, has similar median positioning error with the respect to a system that requires three FTM APs.

## 6 RELATED WORK

Different system designs, that enable a single WiFi node (e.g., an AP) to localize a client, have been proposed. Several techniques require different frequency bands to give the illusion of a wideband radio [2, 20]. SAIL [15] is a ToF system using WiFi that has been designed for localization in multipath environments. SAIL achieved median error of $\approx$ 1m and 80-percentile error of $\approx$ 5 m, which is comparable to our proposed solution, at the drawback of requesting access to inertial sensors in the smartphone and the user intervention to perform calibration steps. Vasisht *et al*. [20] introduced a system that enables a single WiFi AP to localize clients within tens of centimeters. They combine multiple frequency bands scattered around 2.4 GHz and 5 GHz, to obtain almost one GHz of bandwidth. Yet, this approach does not work with commercial of-the-shelf smartphones as they operate on a single frequency channel. In contrast, our proposed solution works with 80 MHz bandwidth and single frequency. Other solutions, as for instance ArrayTrack [22] and SpotFi [12], are based on AOA estimation, and considered a denser AP deployment, which cannot be deployed in home environments and small businesses. [12] deployed 6 APs in an area of 160 $m^2$, for a result of one AP every 26 $m^2$. They achieve a median accuracy of 40 cm, that degrades to 1.6 m in NLOS environments. In contrast, SPRING uses only one AP, with a total of 4 antennas, and it has been deployed in an area of up to 125 $m^2$. There have been many attempts to harness the time-of-flight of wireless signal in indoor propagation environments. Recently, IEEE 802.11-2016 standardized the FTM protocol that has not been well investigated yet. Ibrahim *et al*. [9] conducted different measurements to use and calibrate the RTT provided by the FTM protocol. They achieve in indoor lab and office environments a median error of 5.2 m, using at least three APs. The related work either leverages specialized hardware, combination of multiple frequency bands, a large number of antennas, or multiple APs for trilateration and triangulation. In this paper, we present a solution that employs one single AP, commodity hardware, using a single frequency band and without inputs from inertial sensors.

## 7 CONCLUSION

This paper has presented a hybrid system that methodically addresses many of the challenges towards practical WiFi-based positioning using only a single AP. We have exploited PHY layer information to estimate the direction between the AP and the client using a 802.11ac WiFi chipset that uses 4 linear antennas, operates at 80 MHz and gives access to CSI per sub-carrier. We have presented a phase calibration technique to correct the estimation error introduced by the hardware in the AOA estimations. We have shown how to apply our calibration and the results in the anechoic chamber. Then we have developed an AOA estimator based on channel state information information and we have proposed a methodology to alleviate the effect of multipath in FTM-based ranging using inputs from channel state information. The estimator achieves a median error of 0.5-0.7 meters. Finally we have combined both information, direction and distance between the AP and the STA and have shown for the first time the ability to position a commercial off-the-shelf smartphone only with WiFi measurements performed by one single AP that uses commodity hardware. The experiments have shown a median 2-D positioning error between 0.9 and 2.15 meters in two different testbeds, in areas up to 125 $m^2$ and in presence of strong blockage and multipath.

## 8 ACKNOWLEDGEMENTS

We would like to thank our shepherd Lakshminarayanan Subramanian for his valuable feedback and suggestions. This work has been funded in part by the Madrid Regional Government through TAPIR-CM project S2018/TCS-4496 and in part by Ministerio de Ciencia, Innovación y Universidades (MICIU) grant RTI2018-094313-B-I00 (PinPoint5G+).

# REFERENCES


[1] P. Bahl and V.N. Padmanabhan. 2000. RADAR: an in-building RF-based user location and tracking system. In *Proc. IEEE INFOCOM'00.*

[2] Zhe Chen, Zhongmin Li, Xu Zhang, Guorong Zhu, Yuedong Xu, Jie Xiong, and Xin Wang. 2017. AWL: Turning Spatial Aliasing From Foe to Friend for Accurate WiFi Localization. In *Proceedings of the 13th International Conference on Emerging Networking EXperiments and Technologies (CoNEXT '17)*. ACM, New York, NY, USA, 238–250. https://doi.org/10.1145/3143361.3143377

[3] Krishna Chintalapudi, Anand Padmanabha Iyer, and Venkata N. Padmanabhan. 2010. Indoor localization without the pain. In *In Proc. of ACM MobiCom '10*. 173–184. https://doi.org/10.1145/1859995.1860016

[4] M. Ciurana, F. Barcelo-Arroyo, and F. Izquierdo. 2007. A ranging system with IEEE 802.11 data frames. In *2007 IEEE Radio and Wireless Symposium*. 133–136. https://doi.org/10.1109/RWS.2007.351785

[5] Domenico Giustiniano and Stefan Mangold. 2011. CAESAR: Carrier Sense-based Ranging in Off-the-shelf 802.11 Wireless LAN. In *Proceedings of the Seventh COnference on Emerging Networking EXperiments and Technologies (CoNEXT '11)*. ACM, New York, NY, USA, Article 10, 12 pages. https://doi.org/10.1145/2079296.2079306

[6] Jon Gjengset, Jie Xiong, Graeme McPhillips, and Kyle Jamieson. 2014. Enabling Phased Array Signal Processing on Commodity WiFi Access Points *(Mobicom '14)*. ACM, New York, NY, USA, 12.

[7] Abhishek Goswami, Luis E. Ortiz, and Samir R. Das. 2011. WiGEM: A Learning-based Approach for Indoor Localization *(CoNEXT '11)*. ACM, New York, NY, USA, Article 3, 12 pages. https://doi.org/10.1145/2079296.2079299

[8] Y. Hua and T. K. Sarkar. 1988. Matrix pencil method and its performance. In *ICASSP-88., International Conference on Acoustics, Speech, and Signal Processing*. 2476–2479 vol.4. https://doi.org/10.1109/ICASSP.1988.197145

[9] Mohamed Ibrahim, Hansi Liu, Minitha Jawahar, Viet Nguyen, Marco Gruteser, Richard Howard, Bo Yu, and Fan Bai. 2018. Verification: Accuracy Evaluation of WiFi Fine Time Measurements on an Open Platform. In *Proceedings of the 24th Annual International Conference on Mobile Computing and Networking (MobiCom '18)*. ACM, New York, NY, USA, 417–427. https://doi.org/10.1145/3241539.3241555

[10] IEEE. 2016. IEEE Standard for Information Technology- Telecommunications and Information Exchange Between Systems-Local and Metropolitan Area Networks-Specific Requirements-Part 11: Wireless LAN Medium Access Control (MAC) and Physical Layer (PHY) Specifications. *IEEE Std 802.11-2016 (Revision of IEEE Std 802.11-2012)* (2016), 1–3543.

[11] Sadanori Konishi and Genshiro Kitagawa. 2008. *Information criteria and statistical modeling*. Springer Science & Business Media.

[12] Manikanta Kotaru, Kiran Joshi, Dinesh Bharadia, and Sachin Katti. 2015. SpotFi: Decimeter Level Localization Using WiFi. In *Proceedings of the 2015 ACM Conference on Special Interest Group on Data Communication (SIGCOMM '15)*. ACM, New York, NY, USA, 269–282. https://doi.org/10.1145/2785956.2787487

[13] Hyuk Lim, Lu-Chuan Kung, J.C. Hou, and Haiyun Luo. 2006. Zero-Configuration, Robust Indoor Localization: Theory and Experimentation. In *INFOCOM 2006. 25th IEEE International Conference on Computer Communications. Proceedings*. 1–12. https://doi.org/10.1109/INFOCOM.2006.223

[14] Andreas Marcaletti, Maurizio Rea, Domenico Giustiniano, Vincent Lenders, and Aymen Fakhreddine. 2014. Filtering Noisy 802.11 Time-of-Flight Ranging Measurements. In *Proceedings of the 10th ACM International on Conference on Emerging Networking Experiments and Technologies (CoNEXT '14)*. ACM, New York, NY, USA, 13–20. https://doi.org/10.1145/2674005.2674998

[15] Alex T. Mariakakis, Souvik Sen, Jeongkeun Lee, and Kyu-Han Kim. 2014. SAIL: Single Access Point-based Indoor Localization. In *Proceedings of the 12th Annual International Conference on Mobile Systems, Applications, and Services (MobiSys '14)*. ACM, New York, NY, USA, 315–328. https://doi.org/10.1145/2594368.2594393

[16] D. D. McCrady, L. Doyle, H. Forstrom, T. Dempsey, and M. Martorana. 2000. Mobile ranging using low-accuracy clocks. *IEEE Transactions on Microwave Theory and Techniques* 48, 6 (June 2000), 951–958. https://doi.org/10.1109/22.846721

[17] Anshul Rai, Krishna Kant Chintalapudi, Venkata N. Padmanabhan, and Rijurekha Sen. 2012. Zee: Zero-effort Crowdsourcing for Indoor Localization *(Mobicom '12)*. ACM, New York, NY, USA, 293–304. https://doi.org/10.1145/2348543.2348580

[18] R. Schmidt. 1986. Multiple emitter location and signal parameter estimation. *IEEE Transactions on Antennas and Propagation* 34, 3 (March 1986), 276–280. https://doi.org/10.1109/TAP.1986.1143830

[19] Souvik Sen, Jeongkeun Lee, Kyu-Han Kim, and Paul Congdon. 2013. Avoiding Multipath to Revive Inbuilding WiFi Localization. In *Proceeding of the 11th Annual International Conference on Mobile Systems, Applications, and Services (MobiSys '13)*. ACM, New York, NY, USA, 249–262. https://doi.org/10.1145/2462456.2464463

[20] Deepak Vasisht, Swarun Kumar, and Dina Katabi. 2016. Decimeter-Level Localization with a Single WiFi Access Point. In *13th USENIX Symposium on Networked Systems Design and Implementation (NSDI 16)*. USENIX Association, Santa Clara, CA, 165–178. https://www.usenix.org/conference/nsdi16/technical-sessions/presentation/vasisht

[21] Xinrong Li, K. Pahlavan, M. Latva-aho, and M. Ylianttila. 2000. Comparison of indoor geolocation methods in DSSS and OFDM wireless LAN systems. In *Vehicular Technology Conference Fall 2000. IEEE VTS Fall VTC2000. 52nd Vehicular Technology Conference (Cat. No.00CH37152)*, Vol. 6. 3015–3020 vol.6. https://doi.org/10.1109/VETECF.2000.886867

[22] Jie Xiong and Kyle Jamieson. 2013. ArrayTrack: A Fine-Grained Indoor Location System. In *Presented as part of the 10th USENIX Symposium on Networked Systems Design and Implementation (NSDI 13)*. USENIX, Lombard, IL, 71–84. https://www.usenix.org/conference/nsdi13/technical-sessions/presentation/xiong

[23] Moustafa Youssef and Ashok Agrawala. 2005. The Horus WLAN Location Determination System *(MobiSys '05)*. ACM, New York, NY, USA, 205–218. https://doi.org/10.1145/1067170.1067193